

## Mass transfer and boson cloud depletion in a binary black hole system

Yao Guo, Wenjie Zhong, Yiqiu Ma,<sup>\*</sup> and Daiqin Su<sup>†</sup>

*MOE Key Laboratory of Fundamental Physical Quantities Measurement,  
Hubei Key Laboratory of Gravitation and Quantum Physics, PGMF,  
Institute for Quantum Science and Engineering, School of Physics,  
Huazhong University of Science and Technology, Wuhan 430074, China*



(Received 13 October 2023; accepted 22 April 2024; published 13 May 2024)

The ultralight boson is one of the potential candidates for dark matter. If it exists, it can be generated by a rapidly rotating black hole via superradiance, extracting the energy and angular momentum of the black hole and forming a boson cloud. The boson cloud can be affected by the presence of a companion star, generating rich dynamical effects and producing characteristic gravitational wave signals. During the inspiral of two black holes, the cloud carried with these black holes will redistribute among them and form the so-called black hole molecule. With the framework developed in this work, we analyze the evolution of this black hole molecule and found that bosons occupying the growing modes of the primary black hole can jump to the decaying modes of the companion black hole, resulting in cloud depletion. This mechanism of cloud depletion is different from that induced by the tidal perturbation from the companion.

DOI: [10.1103/PhysRevD.109.104046](https://doi.org/10.1103/PhysRevD.109.104046)

### I. INTRODUCTION

The detection of gravitational waves by current ground-based gravitational wave detectors (LIGO [1], Virgo [2], KAGRA [3], etc.) opens up a new avenue to explore astrophysical processes that involve a strong gravitational field. Future space-borne gravitational wave detectors (LISA [4], TQ [5], Taiji [6], etc.) extend the detection frequency range and allow for exploration of supermassive black holes. One of the interesting target sources for gravitational wave detectors is the ultralight boson, including axion and pseudoscalar axionlike particles. The axion provides a solution to the strong  $CP$  problem [7–9] and has the potential to demystify the baryon asymmetry of the Universe, while more general axionlike particles are predicted by symmetry breaking in string theory [10]. These ultralight bosons are also potential candidates for dark matter [11–15]. The ultralight boson, if it exists, can be produced by a rapidly rotating black hole (BH) through superradiance instabilities [16–24], carrying away the mass and angular momentum of the black hole and forming a boson cloud/condensate [25].

Since the presence of ultralight bosons reduces the mass and spin of the black hole, the precision measurement of black hole mass and spin via gravitational wave detectors provides a powerful constraint on the properties of bosons [26–33]. In addition, the boson cloud can radiate

continuous gravitational waves due to its asymmetric distribution and self-annihilation [25,34], and thus can be detected by future gravitational wave detectors.

If a companion star is present, the boson cloud around a black hole is distorted by a time-dependent tidal field. Under certain conditions, the time-dependent tidal field can induce transitions between the boson's various energy levels, in particular, between the growing modes and the decaying modes [35]. This would generate rich dynamical effects. The transition of the boson can transfer energy and angular momentum from the boson cloud to the companion star, modifying its orbital evolution [36]. In the extreme case, the energy loss of the companion star due to the emission of gravitational waves is balanced by the energy gain from the boson cloud, thus forming the so called “floating orbit” [37]. The modification to the orbital evolution of the binary system can be detected by pulsar timing if the companion star is a pulsar [38,39]. When the boson occupies the decaying mode, it may decay into the black hole, resulting in the depletion of the boson cloud [35,40,41]. In some cases, the boson cloud could be completely cleaned up by the companion star. The bosons that are absorbed by the black hole increase the mass of the black hole while reducing its spin. The reduction of the black hole spin can turn some of the growing modes into decaying modes and then accelerate the cloud depletion [42]. The companion star can also induce transitions between bound and unbound orbits of the boson, and thus ionize it [43]. These dynamical processes of the boson cloud produce characteristic gravitational wave signals and consequently can be detected by current and future gravitational wave

<sup>\*</sup>myqphy@hust.edu.cn

<sup>†</sup>sudaiqin@hust.edu.cn

detectors [44]. This provides a way to infer the presence of the ultralight boson and constrain its properties.

When the black hole and its companion is sufficiently close, the boson can escape to the companion, resulting in a redistribution of the mass of the boson cloud. A gravitational “molecule”, an analog to the hydrogen molecule, can be formed under certain conditions [45,46]. If the companion is also a rotating black hole, then the escaped boson may occupy the decaying modes of the companion black hole and may decay into it. If this happens, then this provides a new channel for boson cloud depletion. In this work, we develop a framework to study the mass transfer between two black holes in a binary system, assuming that the two black holes have the same mass and spin, and their spin orientation is parallel. We make analogy with the hydrogen molecule ion and calculate the wave functions of the molecular orbits and the corresponding energy eigenvalues using the variational method. We then obtain the probability for the boson jumping to the decaying mode of the companion black hole, and show that this leads to a strong cloud depletion which almost completely cleans up the boson cloud.

This paper is organized as follows. In Sec. II, we briefly review the boson cloud around a black hole and its depletion into the black hole due to the time-dependent tidal field produced by the companion. In Sec. III, by making analogy with the hydrogen molecule ion, we use the variational method to derive the wave functions and energy eigenvalues of the boson in the binary black hole system. In Sec. IV, we use the adiabatic approximation to study the time evolution of the wave function of the boson, evaluate the probability of jumping to the decaying mode of the companion black hole, and calculate the time evolution of the cloud mass due to the decay into the companion black hole. We finally conclude in Sec. V. We will use natural units  $\hbar = G = c = 1$  throughout the paper.

## II. BOSON CLOUD AROUND A BLACK HOLE

### A. Gravitational atom

A rapidly rotating black hole can radiate ultralight bosons via superradiance instabilities. These bosons condensate in some of their orbits, forming a boson cloud around the black hole. When the mass of the boson is small, the size of the cloud can be much larger than the gravitational radius of the rotating black hole. In this limit, the Newtonian approximation is sufficient to describe the dynamics of the boson cloud. The orbit of the boson is determined by a Schrödinger-like equation, similar to that of an electron in a hydrogen atom. The eigenstates of the boson are denoted as  $|\varphi_{n\ell m}\rangle$  or  $\varphi_{n\ell m}$ , and the eigenfrequencies are given by [47]

$$\omega_{n\ell m} \approx \mu \left( 1 - \frac{\alpha^2}{2n^2} \right), \quad (1)$$

where  $\mu$  is the mass of the boson,  $\alpha \equiv M\mu$  is the dimensionless “fine-structure constant”. The radial profile of the wave function peaks at

$$r_{c,n} \approx \left( \frac{n^2}{\alpha^2} \right) r_g = n^2 r_b, \quad (2)$$

where  $r_g$  is defined as the gravitational radius of the black hole,  $r_g \equiv M$ , and  $r_b = r_g/\alpha^2$  is defined as the Bohr radius.

However, there is a crucial difference between the electron in the hydrogen atom and the boson around a black hole: the orbits of the electron are stable while the orbits of the boson are not stable due to the presence of the black hole horizon. This is characterized by the imaginary part of the eigenfrequency,  $\omega_{n\ell m} \rightarrow \omega_{n\ell m} + i\Gamma_{n\ell m}$ . In the limit  $\alpha \ll 1$ ,  $\Gamma_{n\ell m}$  can be approximated as [47]

$$\Gamma_{n\ell m} = \frac{2r_+}{M} C_{n\ell m}(\alpha) (m\Omega_H - \omega_{n\ell m}) \alpha^{4\ell+5}, \quad (3)$$

where  $C_{n\ell m}(\alpha)$  is positive and given by

$$C_{n\ell m}(\alpha) = \frac{2^{4\ell+1} (n+\ell)!}{n^{2\ell+4} (n-\ell-1)!} \left[ \frac{\ell!}{(2\ell)!(2\ell+1)!} \right]^2 \times \prod_{j=1}^{\ell} [j^2(1-\tilde{a}^2) + (\tilde{a}m - 2\tilde{r}_+\alpha)^2], \quad (4)$$

with  $\tilde{a} = a/M$  and  $\tilde{r}_+ = r_+/M$ . Here  $r_+$  is the size of the event horizon,  $a$  is the spin and  $\Omega_H$  is the angular velocity of the rotating black hole. The orbits with positive  $\Gamma_{n\ell m}$  are growing modes, for which the number of boson grows exponentially; while the orbits with negative  $\Gamma_{n\ell m}$  are decaying modes, for which the number of boson decays exponentially. Starting from a rapidly rotating black hole, bosons are radiated due to the superradiance instabilities and then occupy the growing modes. The radiated bosons carry away angular momentum, slowing down the rotation of the black hole. At an equilibrium point the black hole rotates slow enough such that no bosons can be further radiated, and a quasi-stationary boson cloud forms around the black hole.

### B. Hyperfine and Bohr resonance

When the black hole with a boson cloud is part of a binary system, the gravitational field of the companion star distorts the cloud, resulting in transition of bosons between growing modes and decaying modes. The bosons that jump to decaying modes can return to the black hole, reducing the total mass of the cloud and transferring angular momentum to the companion star. Therefore, the existence of boson cloud would affect the orbital evolution of the companion star and the gravitational waveforms from the binary system.

The companion star induces a time-dependent perturbation to the Kerr metric, which then introduces a time-dependent shift of gravitational potential to the Schrödinger equation that dominates the dynamics of bosons. Under certain conditions, the time-dependent perturbation can induce resonant transitions between growing modes and decaying modes [35]. There are two types of resonances, the hyperfine (or Rabi) resonance and the Bohr resonance. The resonance occurs at a specific orbital separation. In general, the orbital separation of the hyperfine resonance is much larger than that of the Bohr resonance. This is because the hyperfine energy gap is much narrower than the Bohr energy gap, which implies that the companion star has to be closer to the black hole in order to excite the Bohr resonance.

### III. BOSON ORBITS IN A BINARY BLACK HOLE SYSTEM

We are concerned with the dynamics of the boson cloud when a black hole and its companion are sufficiently close so that mass transfer between them cannot be ignored. It has been shown by using effective field theory techniques [45] and numerical calculation [46] that a gravitational molecule can form in a binary black hole system. Here, we use a simple model to describe the mass transfer and the time evolution of a BH-cloud-companion system. The model is based on the analogy between the hydrogen molecule ion  $H_2^+$  and the BH-cloud-companion system. A similar method is used to study the short-time evolution of the boson cloud in a BH-cloud-pulsar system [48]. Our objective in this work is to describe the full-time evolution of the BH-cloud-companion system, capture the main characteristics of mass transfer and the boson cloud depletion.

For simplicity, we assume: (1) the companion is also a black hole, therefore forming a binary black hole system; (2) two black holes have the same mass and spin; (3) their spin orientation is parallel and perpendicular to the orbital plane. The schematic of the configuration is shown in Fig. 1. These assumptions allow us to focus on the effect of mass transfer, and they can be relaxed to incorporate more complicated effects. Under these assumptions, the orbits of the boson in the BH-cloud-BH system is analogous to that of the electron in the hydrogen molecule ion  $H_2^+$ , except that the two black holes rotate with each other and that the existence of a horizon results in boson absorption.

#### A. Orbits of hydrogen molecule ion

The hydrogen molecule ion  $H_2^+$  consists of two protons and a single electron. The electron moves in the potential produced by the two protons with a fixed distance. The potential is time independent so the electron wave functions can be derived by solving the stationary Schrödinger equation. The approximate energy eigenvalues

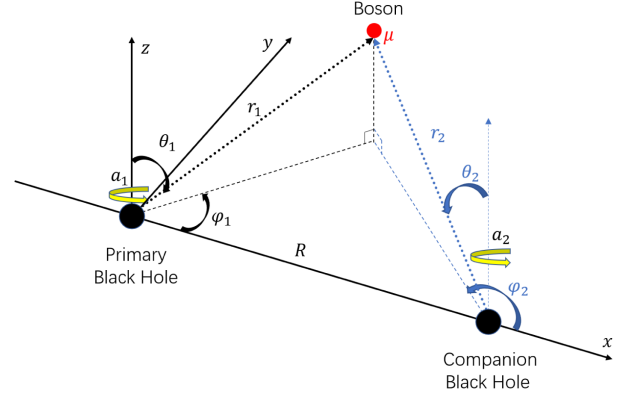


FIG. 1. Configuration of the BH-cloud-BH system and the coordinate system used to describe the boson. The origin of the coordinate system is located at the primary black hole, and the  $z$ -axis is parallel to the spin of the primary black hole and the  $x$ -axis is pointing towards the companion black hole. The spherical coordinates  $(r_1, \theta_1, \varphi_1)$  are used to represent the position of the boson relative to the primary black hole, and  $(r_2, \theta_2, \varphi_2)$  are used to denote the position of the boson relative to the companion black hole. Here  $a_1$  and  $a_2$  represent the spin of the primary and companion black holes, respectively, and  $R$  denotes the orbital separation.

and eigenfunctions can be solved using the variational method. The energy eigenvalues are the stationary points of the expectation value of the Hamiltonian. To approximate the energy eigenvalue, one starts from a trial wave function and then vary the parameters in the trial wave function to find the stationary point of the Hamiltonian.

For the hydrogen molecule ion, the initial trial wave functions can be selected by using the symmetric properties of the system. For example, one can choose a linear superposition of the two ground-state wave functions as a trial function to find the ground state of the hydrogen molecule ion. The excited states can also be found in a similar way.

To maintain the symmetric properties of the system, it is essential to select suitable trial functions in the variational method. Firstly, we employ wave functions  $\varphi_{np_x}$ ,  $\varphi_{np_y}$ , and  $\varphi_{np_z}$  instead of the usual wave functions  $\varphi_{n\ell m}$ , because the former possess symmetric properties that are suitable for constructing molecular orbits. Secondly, for the lowest-order approximation, we linearly superpose wave functions of two isolated hydrogen atoms with the same principal quantum number  $n$ . Therefore, corresponding excited-state molecular orbits can be constructed for each quantum number  $n$ .

In this paper, our main focus is the excited states with  $n = 2$ . This is because a significant fraction of bosons emitted by an isolated rotating black hole through super-radiance occupy the  $n = 2$ ,  $\ell = 1$ , and  $m = 1$  orbits. When a companion black hole is sufficiently close to a primary black hole surrounded by a boson cloud, it is anticipated

that most bosons would occupy the molecular excited states with  $n = 2$ . Other molecular states with a different principal quantum number, e.g.,  $n = 1$ , may also be occupied by bosons; however, the contribution from these molecular orbits is expected to be small, and we neglect them in this paper.

It can be shown that there exists two molecular  $\sigma$  orbits obtained from the atomic orbit  $2p_x$  [49] (see Appendix B for details),

$$\begin{aligned} |\sigma\rangle &= \frac{1}{\sqrt{2N_1}}(|\varphi_{2p_x}^1\rangle - |\varphi_{2p_x}^2\rangle) \\ &= \frac{1}{2N_1}(|\varphi_{2,1,1}^1\rangle + |\varphi_{2,1,-1}^1\rangle - |\varphi_{2,1,1}^2\rangle - |\varphi_{2,1,-1}^2\rangle), \\ |\sigma^*\rangle &= \frac{1}{\sqrt{2N_2}}(|\varphi_{2p_x}^1\rangle + |\varphi_{2p_x}^2\rangle) \\ &= \frac{1}{2N_2}(|\varphi_{2,1,1}^1\rangle + |\varphi_{2,1,-1}^1\rangle + |\varphi_{2,1,1}^2\rangle + |\varphi_{2,1,-1}^2\rangle), \end{aligned} \quad (5)$$

and another two molecular  $\pi$  orbits obtained from the atomic orbit  $2p_y$ ,

$$\begin{aligned} |\pi\rangle &= \frac{1}{\sqrt{2N_3}}(|\varphi_{2p_y}^1\rangle + |\varphi_{2p_y}^2\rangle) \\ &= \frac{1}{2iN_3}(|\varphi_{2,1,1}^1\rangle - |\varphi_{2,1,-1}^1\rangle + |\varphi_{2,1,1}^2\rangle - |\varphi_{2,1,-1}^2\rangle), \\ |\pi^*\rangle &= \frac{1}{\sqrt{2N_4}}(|\varphi_{2p_y}^1\rangle - |\varphi_{2p_y}^2\rangle) \\ &= \frac{1}{2iN_4}(|\varphi_{2,1,1}^1\rangle - |\varphi_{2,1,-1}^1\rangle - |\varphi_{2,1,1}^2\rangle + |\varphi_{2,1,-1}^2\rangle), \end{aligned} \quad (6)$$

where  $N_1$ ,  $N_2$ ,  $N_3$ , and  $N_4$  are introduced to normalize these states,

$$\begin{aligned} N_1 &= \sqrt{1 - \langle\varphi_{2p_x}^1|\varphi_{2p_x}^2\rangle}, & N_2 &= \sqrt{1 + \langle\varphi_{2p_x}^1|\varphi_{2p_x}^2\rangle}, \\ N_3 &= \sqrt{1 + \langle\varphi_{2p_y}^1|\varphi_{2p_y}^2\rangle}, & N_4 &= \sqrt{1 - \langle\varphi_{2p_y}^1|\varphi_{2p_y}^2\rangle}. \end{aligned} \quad (7)$$

It is evident that  $N_i$  depends on the distance between two protons. In the following, we will use the notation  $i = 1, 2, 3, 4$  to denote the four molecular orbits  $\sigma, \sigma^*, \pi,$  and  $\pi^*$ , respectively.

## B. Born-Oppenheimer approximation

We now turn to the problem of solving the orbits of the boson in a binary black hole system with the two black holes have the same mass and spin. This system is analogous to the hydrogen molecule ion  $\text{H}_2^+$  except that the two black holes rotate with each other and their separation shrinks due to the emission of gravitational

waves. The bosons experience a time-dependent field rather than a static one. An important question is how to take into account the effects of rotation and orbital shrinking.

In Ref. [35], the rotation of the companion star relative to the primary black hole produces a time-dependent perturbation to the primary black hole, which then induces hyperfine and Bohr mixing of growing and decaying modes, resulting in boson cloud depletion. Whilst we are concerned with the transfer of bosons between the two black holes, the framework developed in Ref. [35] does not apply here. As a first approximation, we neglect the effects of rotation and orbital shrinking, and treat the two black holes as stationary with a fixed orbital separation. This is known as the Born-Oppenheimer approximation, in which the binary black hole system with a boson cloud is analogous to the hydrogen molecule ion at any given time. Before performing the detailed calculation, we compare various timescales to validate the use of Born-Oppenheimer approximation.

The velocity of a boson can be estimated using the Virial theorem and the uncertainty principle. The boson's velocity  $v_a$  satisfies,

$$\frac{1}{2}\mu v_a^2 \sim \frac{M\mu}{r_c}, \quad \mu v_a \sim \frac{1}{r_c}, \quad (8)$$

where  $r_c$  is the typical length scale of the radial profile of the boson cloud. This implies

$$v_a \sim M\mu \sim \alpha. \quad (9)$$

The relaxation timescale for the boson can be approximated by

$$\tau_r \sim \frac{R}{v_a} \sim \frac{R}{\alpha}. \quad (10)$$

The time  $\tau_r$  characterizes the timescale for the boson moving from one black hole to the other. The period of the binary black holes is simply given by

$$T = \frac{2\pi}{\Omega} = 2\pi\sqrt{\frac{R^3}{M(1+q)}}. \quad (11)$$

Therefore the ratio between  $\tau_r$  and  $T$  is

$$\frac{\tau_r}{T} \sim \frac{\sqrt{1+q}}{2\pi} \sqrt{\frac{M}{\alpha^2 R}} \sim \frac{\sqrt{1+q}}{2\pi} \sqrt{\frac{r_b}{R}}. \quad (12)$$

For  $q = 1$  and  $R = 32r_b$ ,  $\tau_r/T \sim 1/8\pi \sim 0.04$ . As we will see in the following discussion, the mass transfer occurs when  $R \gtrsim 50r_b$ . This shows that for an intermediate orbital separation, the relaxation time of the boson is

much shorter than the period of the binary. Therefore, the two black holes can be treated as quasistatic when considering the transfer of bosons and the Born-Oppenheimer approximation applies.

The orbit of the binary black holes shrinks due to the emission of gravitational waves [50],

$$R(t) = \left[ \frac{M(1+q)}{\Omega_0^2} \right]^{1/3} \left( -\frac{t}{\tau_0} \right)^{1/4}, \quad (13)$$

where we set  $t = 0$  as the moment of merger, and  $\tau_0$  is the time to merger for an initial orbital frequency  $\Omega_0$ . The initial time  $\tau_0$  and initial orbital frequency  $\Omega_0$  are related via

$$\frac{\tau_0}{M(1+q)} = \frac{5}{256} \frac{(1+q)^2}{q} \left[ \frac{1}{M(1+q)\Omega_0} \right]^{8/3}. \quad (14)$$

The characteristic timescale for coalescence can be estimated via

$$\tau_p = \left| \left( \frac{dR}{dt} \right)^{-1} \right|_{R \approx \frac{5}{64} \frac{R^4}{M^3} \frac{1}{q(1+q)}}. \quad (15)$$

This timescale is evidently much longer than the period of the binary  $T$ , and it is thus also much longer than the boson relaxation timescale  $\tau_r$ ,

$$\frac{\tau_r}{\tau_p} \sim \frac{32}{5} \alpha^5 \left( \frac{r_b}{R} \right)^3 q(1+q). \quad (16)$$

When the orbital separation of the two black holes is sufficiently large and  $q$  is not so large, these two ratios are both much smaller than one, so the Born-Oppenheimer approximation is sound.

### C. Eigenfunctions and energy eigenvalues

To find the exact eigenfunctions and eigenfrequencies, one in principle needs to solve the Klein-Gordon equation of the boson in the background spacetime of the binary black hole system, which is quite a challenging task. When the mass of the boson is small, the boson cloud is far away from the black hole and Newtonian approximation can be used to derive the eigenfunctions [35]. To the order of  $1/r$ , the wave function of the boson around a single rotating black hole satisfies,

$$i\hbar \frac{\partial}{\partial t} \psi(t, \mathbf{r}) = \left( -\frac{1}{2\mu} \nabla^2 - \frac{\alpha}{r} \right) \psi(t, \mathbf{r}), \quad (17)$$

which is exactly in the same form as the Schrödinger equation for the electron in a hydrogen atom. When the two black holes are not so close to each other and the boson lingers around a regime far away from both black holes, then the Newtonian approximation applies. To the order of  $1/r$ , the wave function of the boson in the binary black hole system satisfies,

$$i\hbar \frac{\partial}{\partial t} \psi(t, \mathbf{r}) = \left( -\frac{1}{2\mu} \nabla^2 - \frac{\alpha}{r_1} - \frac{\alpha}{r_2} \right) \psi(t, \mathbf{r}), \quad (18)$$

where  $r_1$  is the distance between the boson and the primary black hole, and  $r_2$  is the distance between the boson and the companion black hole. Equation (18) is exactly in the same form as the Schrödinger equation for the electron in the hydrogen molecule ion, without including the interaction between two protons.

In the Born-Oppenheimer approximation, the eigenfunctions of the boson at any given time can be derived straightforwardly. They are exactly in the same form as those given by Eqs. (5) and (6), with  $|\varphi_{n\ell m}\rangle$  the eigenfunctions of the boson in a single isolated rotating black hole. Furthermore, the normalization constants  $N_i$  depend on the configuration of the BH-cloud-BH system. For the case that we consider here, the normalization constants have no analytic expressions and are needed to be evaluated numerically.

Once the eigenfunctions are known, the energy eigenvalues can be calculated straightforwardly, which are simply the expectation values of the Hamiltonian. From Eq. (18) it is evident that the Hamiltonian of the boson in the Newtonian limit is

$$\hat{H} = -\frac{1}{2\mu} \nabla^2 - \frac{\alpha}{r_1} - \frac{\alpha}{r_2}. \quad (19)$$

To simplify the calculation, we divide the Hamiltonian  $\hat{H}$  into two parts; the Hamiltonian of the boson in the primary black hole and the potential produced by the companion black hole, namely,  $\hat{H} = \hat{H}_1 - \frac{\alpha}{r_2}$  with  $\hat{H}_1 = -\frac{1}{2\mu} \nabla^2 - \frac{\alpha}{r_1}$ . The Hamiltonian can also be expressed as  $\hat{H} = \hat{H}_2 - \frac{\alpha}{r_1}$  with  $\hat{H}_2 = -\frac{1}{2\mu} \nabla^2 - \frac{\alpha}{r_2}$ . Since the two black holes have equal mass, the energy eigenvalues and eigenfunctions for  $\hat{H}_1$  and  $\hat{H}_2$  are the identical. We will leverage this symmetry to further simplify the calculation of the energy eigenvalues of the Hamiltonian  $\hat{H}$ , which are given by

$$\begin{aligned}
 E_1 &= \langle \sigma | \hat{H} | \sigma \rangle = \frac{1}{N_1^2} \left[ -\frac{1}{8} \mu \alpha^2 (1 - \langle \varphi_{2p_x}^1 | \varphi_{2p_x}^2 \rangle) - \langle \varphi_{2p_x}^1 | \frac{\alpha}{r_2} | \varphi_{2p_x}^1 \rangle + \langle \varphi_{2p_x}^1 | \frac{\alpha}{r_2} | \varphi_{2p_x}^2 \rangle \right], \\
 E_2 &= \langle \sigma^* | \hat{H} | \sigma^* \rangle = \frac{1}{N_2^2} \left[ -\frac{1}{8} \mu \alpha^2 (1 + \langle \varphi_{2p_x}^1 | \varphi_{2p_x}^2 \rangle) - \langle \varphi_{2p_x}^1 | \frac{\alpha}{r_2} | \varphi_{2p_x}^1 \rangle - \langle \varphi_{2p_x}^1 | \frac{\alpha}{r_2} | \varphi_{2p_x}^2 \rangle \right], \\
 E_3 &= \langle \pi | \hat{H} | \pi \rangle = \frac{1}{N_3^2} \left[ -\frac{1}{8} \mu \alpha^2 (1 + \langle \varphi_{2p_y}^1 | \varphi_{2p_y}^2 \rangle) - \langle \varphi_{2p_y}^1 | \frac{\alpha}{r_2} | \varphi_{2p_y}^1 \rangle - \langle \varphi_{2p_y}^1 | \frac{\alpha}{r_2} | \varphi_{2p_y}^2 \rangle \right], \\
 E_4 &= \langle \pi^* | \hat{H} | \pi^* \rangle = \frac{1}{N_4^2} \left[ -\frac{1}{8} \mu \alpha^2 (1 - \langle \varphi_{2p_y}^1 | \varphi_{2p_y}^2 \rangle) - \langle \varphi_{2p_y}^1 | \frac{\alpha}{r_2} | \varphi_{2p_y}^1 \rangle + \langle \varphi_{2p_y}^1 | \frac{\alpha}{r_2} | \varphi_{2p_y}^2 \rangle \right].
 \end{aligned} \tag{20}$$

For the case that we consider here, there exists no analytic expressions for  $E_i$ , so they have to be evaluated numerically. Note that in deriving the eigenfunctions and energy eigenvalues, we have ignored the higher-order corrections to the Hamiltonian. This results in degeneracy of all four energy levels when the two black holes are infinitely far away.

#### IV. CLOUD DEPLETION

Assume that the primary black hole has a boson cloud surrounding it while the companion black hole does not. When the two black holes are very far away from each other, the bosons move around the primary black hole and cannot escape to the companion. When the two black holes become closer to each other, the boson orbits that belong to the primary black hole and that belong to the companion have more overlap, forming boson orbits that are analogous to the molecular orbits of the hydrogen molecule ion. Therefore, the boson around the primary black hole may jump to the companion. This can have two consequences; first, the bosons redistribute in the binary black hole system, changing its quadrupole and thus modifying the gravitational waveform, and second, the bosons may jump to the decaying modes of the companion, and therefore could be absorbed by the companion black hole. To estimate the importance of the above two consequences, one needs to model the process of boson transfer from the primary black hole to its companion.

The binary black hole system emits gravitational waves so its orbit shrinks, namely, the orbital separation between the two black holes shrinks due to the radiation of energy. The orbital separation, denoted as  $R(t)$ , is thus time dependent. This implies that the eigenfunctions and eigenfrequencies are also time dependent because they are solved at a given time assuming the orbital separation is fixed. These solutions are meaningful only in the case where the timescale of the orbital shrinking is much larger than that of the boson relaxation. This is exactly the case as we have discussed in Sec. III B. In order to know the evolution of the boson cloud in the binary black hole system, one needs to solve a time-dependent Schrödinger equation, in which the Hamiltonian varies slowly. This sort of problem can be solved using the adiabatic approximation

if the energy levels are not degenerate and the energy gap is sufficiently large.

#### A. Adiabatic approximation

We numerically calculate the energy eigenvalues given by Eq. (20) and plot them in Figs. 2 and 3. It can be seen from Fig. 2 that the four energy levels split and the energy gap is larger when the two black holes are closer. The gap

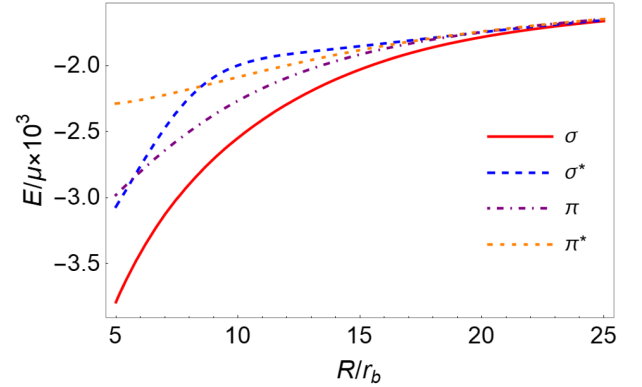


FIG. 2. Energy eigenvalues of the boson molecular orbits for small orbital separation. Here we choose  $q = 1$  and  $\alpha = 0.1$  as an example.

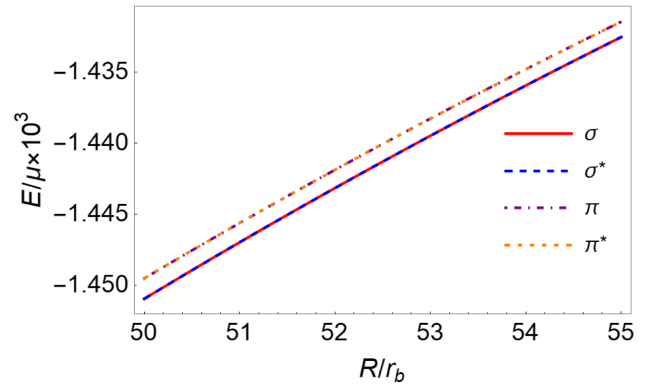


FIG. 3. Energy eigenvalues of the boson molecular orbits for large orbital separation. Here we choose  $q = 1$  and  $\alpha = 0.1$  as an example.

decreases as the orbital separation increases, which is consistent with the fact that the four energy levels are degenerate when  $R \rightarrow \infty$ . Figure 3 shows that the energy gaps between orbits  $\sigma$  and  $\sigma^*$ , and orbits  $\pi$  and  $\pi^*$  decrease much faster than that between  $\sigma$ 's and  $\pi$ 's orbits. Because the energy gaps between orbits  $\sigma$  and  $\sigma^*$ , and orbits  $\pi$  and  $\pi^*$  are very close, a question arises as to whether the adiabatic approximation is still valid.

In the adiabatic approximation, the eigenfunctions and energy eigenvalues vary slowly with time, but the boson remains in the initial energy level during the subsequent evolution, namely, no transition from one energy level to others. In order to see whether the adiabatic approximation is valid for the problem we consider here, we need to check whether the transition between orbits  $\sigma$  and  $\sigma^*$ , and orbits  $\pi$  and  $\pi^*$  is negligible.

Consider an arbitrary quantum state,

$$|\psi(t)\rangle = \sum_n c_n(t) |\psi_n(t)\rangle, \quad (21)$$

where  $|\psi_n(t)\rangle$  and  $c_n(t)$  are the time-dependent energy eigenstates and their corresponding coefficients, respectively. In the adiabatic approximation, we have  $|c_n(t+dt)| = |c_n(t)|$ , namely, there is no transition between different energy levels. To estimate the accuracy of the adiabatic approximation, one can check the amplitude of the time derivative of the coefficient  $c_n(t)$ . It can be shown that (see Appendix C for details),

$$\frac{dc_k}{dt} = -\sum_{n \neq k} c_n \frac{1}{E_n - E_k} \langle \psi_k | \frac{\partial \hat{H}}{\partial t} | \psi_n \rangle - ic_k E_k, \quad (22)$$

where the summation characterizes the transition from the initial energy level to other energy levels, and the last term represents the free evolution in the initial energy level. Now consider the set of state  $\{|\psi_k\rangle\}$  as the four orbits  $|\sigma\rangle, |\sigma^*\rangle, |\pi\rangle$  and  $|\pi^*\rangle$ . Due to the symmetry of the system, it can be shown (see Appendix C for details) that

$$\langle \psi_k | \frac{\partial \hat{H}}{\partial t} | \psi_n \rangle = 0, \quad (23)$$

for  $n \neq k$ . This implies that the adiabatic approximation is a good approximation to the time evolution of the boson. Under the adiabatic approximation, the time derivative of the coefficient  $c_k$  is given by  $\dot{c}_k = -ic_k E_k$ . Therefore, the solution of the coefficient  $c_k$  is  $c_k(t) = c_k(t_0) e^{-i \int_{t_0}^t E_k(\tau) d\tau}$  and the state  $|\psi(t)\rangle$  evolves as

$$|\psi(t)\rangle = \sum_n c_n(t_0) e^{-i \int_{t_0}^t E_n(\tau) d\tau} |\psi_n(t)\rangle, \quad (24)$$

where  $t_0$  is the initial time.

Taking into account the emission of gravitational waves and the orbital shrinking, the energy eigenvalues and eigenstates are all time dependent, denoted as  $E_i(t)$ ,  $|\sigma(t)\rangle, |\sigma^*(t)\rangle, |\pi(t)\rangle$  and  $|\pi^*(t)\rangle$ , respectively. When the two black holes are infinitely far away, namely,  $t \rightarrow -\infty$  and  $R \rightarrow \infty$ , the normalization constants defined in Eq. (7) are the same and equal to one. This implies that the initial state of the boson can be written as

$$\begin{aligned} |\Phi(-\infty)\rangle &\equiv |\varphi_{2,1,1}^1\rangle \\ &= \frac{1}{2} [|\sigma(-\infty)\rangle + |\sigma^*(-\infty)\rangle \\ &\quad + i|\pi(-\infty)\rangle + i|\pi^*(-\infty)\rangle]. \end{aligned} \quad (25)$$

From Eq. (24) the subsequent evolution of the state is

$$\begin{aligned} |\Phi(t)\rangle &= \frac{1}{2} \left[ e^{-i \int_{-\infty}^t E_1(\tau) d\tau} |\sigma\rangle + e^{-i \int_{-\infty}^t E_2(\tau) d\tau} |\sigma^*\rangle \right. \\ &\quad \left. + i e^{-i \int_{-\infty}^t E_3(\tau) d\tau} |\pi\rangle + i e^{-i \int_{-\infty}^t E_4(\tau) d\tau} |\pi^*\rangle \right], \end{aligned} \quad (26)$$

We now substitute Eqs. (5) and (6) into Eq. (26) and obtain an expansion of  $|\Phi(t)\rangle$  in terms of the isolated orbits  $|\varphi_{2,1,\pm 1}^1\rangle$  and  $|\varphi_{2,1,\pm 1}^2\rangle$ . The coefficient of the state  $|\varphi_{2,1,-1}^2\rangle$  is given by

$$\begin{aligned} C_-(t) &= -\frac{1}{4N_1} e^{-i \int_{-\infty}^t E_1(\tau) d\tau} + \frac{1}{4N_2} e^{-i \int_{-\infty}^t E_2(\tau) d\tau} \\ &\quad - \frac{1}{4N_3} e^{-i \int_{-\infty}^t E_3(\tau) d\tau} + \frac{1}{4N_4} e^{-i \int_{-\infty}^t E_4(\tau) d\tau}. \end{aligned} \quad (27)$$

The nonzero overlap between the isolated orbit  $|\varphi_{2,1,-1}^2\rangle$  and  $|\Phi(t)\rangle$  implies that bosons can jump to the orbits of the companion black hole during their evolution. The modular square of  $C_-(t)$ ,

$$\begin{aligned} |C_-(t)|^2 &= \sum_i \frac{1}{16N_i^2} \\ &\quad + \sum_{i < j} (-1)^{i+j} \frac{1}{8N_i N_j} \cos \left[ \int_{-\infty}^t (E_i(\tau) - E_j(\tau)) d\tau \right], \end{aligned} \quad (28)$$

represents the probability of jumping to the isolated orbit  $|\varphi_{2,1,-1}^2\rangle$ . If we only consider the effect of gravitational wave emission and neglect other effects like back reaction of the boson cloud onto the orbital evolution, then we can use the relation defined in Eq. (13) to express the coefficient as a function of  $R$ , namely,  $C_-(R)$ , and the time integration in Eq. (28) can be replaced by an integration over the orbital separation  $R$ .

When  $R$  is sufficiently large, the energy levels of orbits  $\sigma$  and  $\sigma^*$  are almost degenerate ( $E_1 \approx E_2$ ), as well as that of orbits  $\pi$  and  $\pi^*$  ( $E_3 \approx E_4$ ), as can be seen from Fig. 3.

In addition, the normalization factors satisfy  $N_1(R) \approx N_2(R)$  and  $N_3(R) \approx N_4(R)$ . This implies that the coefficient  $C_-(R)$  approaches to zero when the two black holes are sufficiently far away from each other, which is consistent with the fact that the boson cannot escape to a companion that is very far away. When the two black holes are closer, the energy levels of orbits  $\sigma$  and  $\sigma^*$  become nondegenerate ( $E_1 \neq E_2$ ), as well as those of orbits  $\pi$  and  $\pi^*$ . The coefficient  $C_-(R)$  gradually becomes nonzero, indicating that the boson can transfer to the companion black hole. From Eq. (28) we can see that the probability  $|C_-(R)|^2$  is the sum of six oscillating terms having frequencies  $|E_i - E_j|$ , with  $i, j = \{\sigma, \sigma^*, \pi, \pi^*\}$ . The frequencies  $|E_i - E_j|$  with  $i \in \{\sigma, \sigma^*\}$  and  $j \in \{\pi, \pi^*\}$ , or  $j \in \{\sigma, \sigma^*\}$  and  $i \in \{\pi, \pi^*\}$ , are much higher than that when  $i, j \in \{\sigma, \sigma^*\}$  or  $i, j \in \{\pi, \pi^*\}$ .

Figure 4 shows the occupation probability  $|C_-(R)|^2$  of the orbit  $|\psi_{2,1,-1}^2\rangle$ , which is one of the decaying modes of the companion black hole. In the numerical calculation, we use a sufficiently large distance  $R = 80r_b$  as a replacement for the infinitely large distance ( $t = -\infty$ ) in the lower limit of the integration in Eq. (28), which introduces a negligible error. The blue curve takes into account the full expression of  $|C_-(R)|^2$  and includes highly oscillating terms, as shown by Fig. 5. If we remove the highly oscillating terms and only keep two terms with oscillating frequencies  $|E_\pi - E_{\pi^*}|$  and  $|E_\sigma - E_{\sigma^*}|$ , we obtain the profile of the probability  $|C_-(R)|^2$ , which is the orange curve shown in Fig. 4. The profile captures the change of the probability that the boson occupies the decaying mode of the companion black hole during the evolution of the binary black holes. When  $R > 63r_b$ , the probability is almost zero. It gradually increases as  $R$  decreases and reaches its first maximum around  $R = 55.5r_b$ . The first maximum of the probability is about 0.3, showing that a significant amount of boson

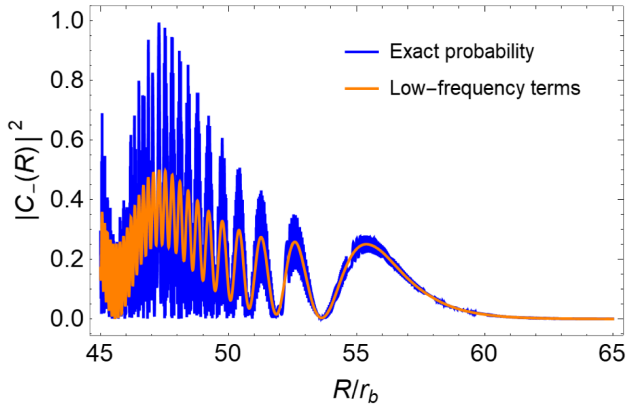


FIG. 4. Probability for a boson jumping to the decaying mode  $|\psi_{2,1,-1}^2\rangle$  of the companion black hole. Here we choose  $q = 1$  and  $\alpha = 0.1$ . The blue curve includes both the rapidly oscillating and slowly oscillating terms, while the orange curve includes only the slowly oscillating terms.

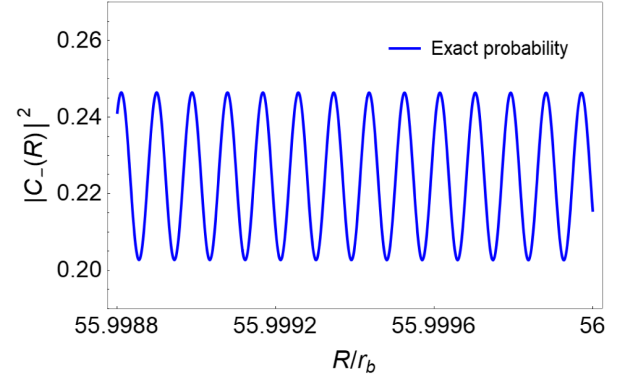


FIG. 5. High-frequency oscillations of the probability for a boson transitioning to the decaying mode  $|\psi_{2,1,-1}^2\rangle$  of the companion black hole. We have chosen orbital separations around  $R = 56r_b$ .

transfers to the companion black hole and occupies the decaying mode  $|\psi_{2,1,-1}^2\rangle$ . As the orbital separation  $R$  further decreases, the profile of the probability oscillates with a higher and higher frequency. Note that the orbital separation corresponding to the first maximum is larger than the Roche limit, which is about  $10r_b$  for  $q = 1$ .

We now consider the scenario where the companion black hole also possesses a boson cloud. Since initially the two black holes are very far away, the process of super-radiance in each black hole is independent and uncorrelated. The state of a boson is therefore an incoherent mixture of the state  $|\varphi_{2,1,1}^1\rangle$  with probability  $p_1$  and the state  $|\varphi_{2,1,1}^2\rangle$  with probability  $p_2$ , namely, the state of a boson is described by an ensemble  $\{|\varphi_{2,1,1}^1\rangle, p_1; |\varphi_{2,1,1}^2\rangle, p_2\}$ . The probability  $p_1$  and  $p_2$  can be determined by the initial mass of the boson clouds surrounding the two black holes. In this paper, we neglect the interaction between boson clouds so the boson evolves only under the influence of the other black hole. Therefore, the evolution of the state of the boson in the companion black hole can be derived in a similar way. The initial state of the boson can be written as

$$\begin{aligned} |\Psi(-\infty)\rangle &\equiv |\varphi_{2,1,1}^2\rangle \\ &= \frac{1}{2} [|\sigma^*(-\infty)\rangle - |\sigma(-\infty)\rangle \\ &\quad + i|\pi(-\infty)\rangle - i|\pi^*(-\infty)\rangle]. \end{aligned} \quad (29)$$

According to the adiabatic approximation, the subsequent evolution of the state is

$$\begin{aligned} |\Psi(t)\rangle &= \frac{1}{2} \left[ -e^{-i \int_{-\infty}^t E_1(\tau) d\tau} |\sigma\rangle + e^{-i \int_{-\infty}^t E_2(\tau) d\tau} |\sigma^*\rangle \right. \\ &\quad \left. + i e^{-i \int_{-\infty}^t E_3(\tau) d\tau} |\pi\rangle - i e^{-i \int_{-\infty}^t E_4(\tau) d\tau} |\pi^*\rangle \right], \end{aligned} \quad (30)$$

We now substitute Eqs. (5) and (6) into Eq. (30) and obtain an expansion of  $|\Psi(t)\rangle$  in terms of the isolated orbits



$|\varphi_{2,1,\pm 1}^1\rangle$  and  $|\varphi_{2,1,\pm 1}^2\rangle$ . It is straightforward to show that the coefficient of the state  $|\varphi_{2,1,-1}^1\rangle$  is the same as  $C_-(t)$  given by Eq. (27). This is expected due to the symmetry of the system.

The boson occupying the decaying mode may decay into the black hole, resulting in the depletion of the boson cloud. The boson that transfers to the decaying mode of the companion therefore may decay into the companion black hole. This is another channel other than the hyperfine mixing and Bohr mixing that could result in cloud depletion. Assuming that the backreaction is small and the decay rate of the black hole is not affected by the presence of another black hole, the time evolution of the cloud mass can be described as

$$\frac{dM_c}{dt} = 2 \sum_{i=1}^2 \Gamma_{2,1,-1} |C_{2,1,-1}^i|^2 M_c, \quad (31)$$

where  $M_c$  is the mass of the boson cloud and  $\Gamma_{2,1,-1}$ , defined by Eq. (3), is the decay rate of the decaying mode  $|\psi_{2,1,-1}\rangle$ . Here  $|C_{2,1,-1}^1|^2$  is the occupation probability of the decaying mode  $|\psi_{2,1,-1}^1\rangle$  of the primary black hole and  $|C_{2,1,-1}^2|^2$  is the occupation probability of the decaying mode  $|\psi_{2,1,-1}^2\rangle$  of the companion black hole, namely,  $|C_{2,1,-1}^2|^2 = |C_-(R)|^2$ . The summation takes into account the decay of the boson into both the primary and companion black holes.

To see the effect of mass transfer onto the cloud depletion, we calculate the time evolution of the cloud mass under the assumption that the bosons only decay into the companion black hole. Suppose the total mass of the cloud right before the boson escapes to the companion, e.g.,  $R = 80r_b$ , is  $M_{c,0}$ . We further assume that the spin of the two black holes are both  $\chi = \frac{4\alpha}{1+4\alpha^2}$ , which is the critical spin for  $|\varphi_{2,1,1}\rangle$  to be saturated [21,25,51], and the companion black hole has no bosons around it (otherwise, we have to modify the initial state of the cloud, which can also be handled in our framework). Backreaction of the boson cloud onto the black holes are neglected. The result is shown as the blue dashed curve in Fig. 6. We can see that the boson cloud quickly decays around  $R = 60r_b$  and finally almost all bosons are absorbed by the companion black hole. To be more specific, the cloud remains unchanged when  $R \gtrsim 67r_b$  and almost completely disappears when  $R \lesssim 57r_b$ . This means all bosons decay into the companion black hole when the probability  $|C_-(R)|^2$  is approaching to its first maximum. At first glance this seems impossible because the maximal probability is about 0.3, which is smaller than one. From the physical perspective this is reasonable. Each boson moves between the primary and companion black holes. It may be absorbed by the companion black hole when it occupies the orbit  $|\varphi_{2,1,-1}\rangle$  of the companion. Though the probability of being absorbed

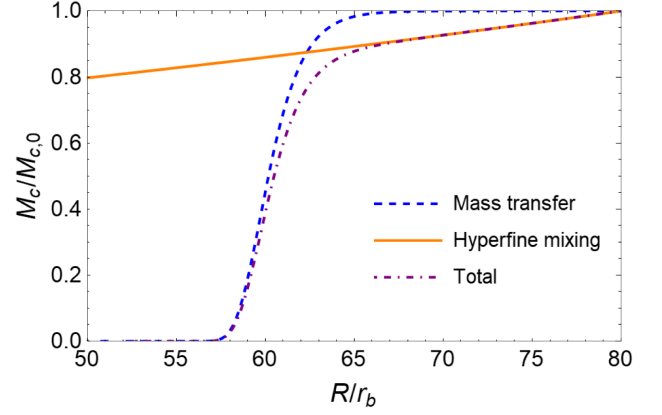


FIG. 6. Evolution of the boson cloud mass for  $\alpha = 0.1$ . The blue dashed curve denotes the cloud depletion due to the mass transfer to the decaying mode of the companion black hole, the orange curve denotes the cloud depletion due to the hyperfine mixing of the boson in the primary black hole and the purple dashed-dotted curve denotes the total cloud depletion.

within one round trip is quite small, the boson can travel many round trips when the orbital separation decreases from  $67r_b$  to  $57r_b$ . Therefore, with a very high probability, the boson has been absorbed by the companion black hole when  $R < 57r_b$ . This is also the key difference from the depletion mechanism due to the hyperfine resonance. It is true that at the resonance point, nearly all bosons jump to the decaying mode, however, the bosons stay in the decaying mode only for a short time, so the total mass that absorbed by the black hole may not be large, as demonstrated in Ref. [35].

We can also include the cloud depletion due to the hyperfine mixing. Instead of directly calculating the coefficients of the orbits  $|\varphi_{2,1,\pm 1}^1\rangle$  from Eq. (26), we use the method developed in Ref. [35] to calculate the probability that the boson jumps to the decaying mode of the primary black hole due to the perturbation of the companion black hole. Firstly, the effect of rotation is not included in Eq. (26). Secondly, according to the adiabatic theorem, the slow orbital shrinking cannot induce a direct transition from the growing mode  $|\varphi_{2,1,1}^1\rangle$  to the decaying mode  $|\varphi_{2,1,-1}^1\rangle$  of the primary black hole. A boson may jump to the decaying mode  $|\varphi_{2,1,-1}^1\rangle$  by first moving to the companion black and then back to the primary black hole. However, this is a second order effect and the probability is at the order of  $|C_-(R)|^4$ , which therefore can be neglected.

For the parameters that we consider in this paper, the hyperfine resonance occurs at the orbital separation  $R \approx 660r_b$ , which is much larger than the orbital separation where the mass transfer occurs. It is therefore expected that the cloud depletion due to the hyperfine mixing is slower than that due to the mass transfer in the regime  $R < 80r_b$ , which is confirmed by Fig. 6. The reason is that the probability for a boson jumping to the decaying mode of

the primary black hole is very small in this regime. Combining the effects of the mass transfer and hyperfine mixing together, we obtain the total cloud depletion, which is shown in Fig. 6. When  $R \gtrsim 67r_b$ , the depletion is mostly contributed by the hyperfine mixing and when  $R \lesssim 67r_b$ , the depletion is mostly contributed by the mass transfer to the companion black hole and the decay into it. At about  $R \sim 57r_b$ , the cloud has completely decayed into the two black holes, which is much earlier than the prediction of hyperfine mixing alone.

In the above discussion we assume that a boson cloud exists when the orbital separation is about  $R = 80r_b$ . This could happen in several cases. The boson cloud may form when the two black holes are close enough, in particular, when the orbital separation is much smaller than the orbit separation when the hyperfine resonance occurs. In this case the cloud depletes very slowly due to the hyperfine mixing and a significant amount of bosons may still remain when the mass transfer starts to contribute to the depletion. The boson cloud may also form when the two black holes are very far away, in particular, when the orbital separation is larger than the orbit separation when the hyperfine resonance occurs. There are two possibilities in this case. If the companion black hole and the cloud are counter-rotating, then the hyperfine resonance never occurs. The hyperfine and Bohr mixing are both weak so the cloud depletes very slowly, as shown in Fig. 7, and therefore a substantial amount of cloud may still remain. If the companion black hole and the cloud are corotating, then the hyperfine resonance occurs. The hyperfine resonance may cause a strong depletion of the cloud so that only a small amount of cloud is left when the mass transfer starts to contribute to the depletion. If this is the case, then the effect of mass transfer does not play an important role in the cloud depletion.

As an example, we consider the case where the companion black hole and the cloud are corotating, and the cloud forms after the hyperfine resonance occurs.

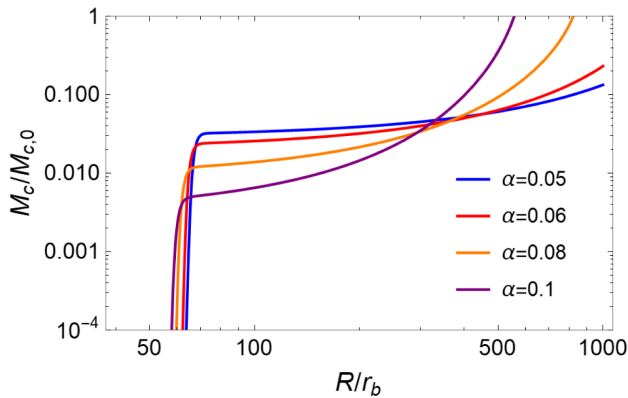


FIG. 7. Evolution of the boson cloud mass for different  $\alpha$  and initial cloud mass  $M_{c,0} = \alpha M$  [26].

The cloud has a life time  $\tau_c$  that determined only by its own gravitational radiation, which is given by [26,35,52]

$$\tau_c \sim 10^7 \left( \frac{M}{3M_\odot} \right) \left( \frac{0.07}{\alpha} \right)^{15} \text{ years}, \quad (32)$$

where  $M$  is the mass of the primary black hole. We set the initial time of the cloud evolution as the half-lifetime of the cloud. The results are shown in Fig. 7, where we have included the contribution from the hyperfine mixing, Bohr mixing, mass transfer, and gravitational radiation by the cloud itself. For a fixed value of  $\alpha$ , the cloud depletion due to the hyperfine mixing, Bohr mixing and gravitational radiation dominates at large orbital separation, which proceeds very slowly. When the two black holes are close enough and the mass transfer occurs, the cloud quickly depletes and almost all remaining bosons are absorbed by the companion black hole. For a smaller value of  $\alpha$ , the cloud depletes slower during the stage of hyperfine mixing and the mass transfer occurs earlier, i.e., at a larger orbital separation. This implies that a larger fraction of boson depletes due to the mass transfer and is absorbed by the companion black hole.

## B. Modification to gravitational radiation

The mass transfer and cloud depletion change the mass distribution of the BH-cloud-BH system, consequently affecting the radiated gravitational waves. The power of gravitational radiation emitted by a system is related to the third time derivative of its quadrupole moment via

$$\frac{dE_{\text{GW}}}{dt} = \frac{1}{5} \sum_{i,j=1}^3 \ddot{Q}_{ij} \ddot{Q}_{ij}, \quad (33)$$

where the quadrupole moment  $Q_{ij}$  is defined as

$$Q_{ij} = \int d^3x \rho(x) \left( x_i x_j - \frac{1}{3} x^2 \delta_{ij} \right), \quad (34)$$

with  $\rho(x)$  the mass density distribution. In a binary black hole system without a boson cloud, the two black holes can be approximated as two point masses if their gravitational radii are much smaller than their orbital separation. In this approximation, it is straightforward to show that the average radiation power is given by

$$P_0 = \frac{32}{5} \left( \frac{M_1 M_2}{M_1 + M_2} \right)^2 R^4 \Omega^6, \quad (35)$$

where  $M_1$  and  $M_2$  represent the black hole masses,  $R$  is the orbital separation and  $\Omega$  is the orbital (assuming circular orbit) frequency.

When a boson cloud forms around the primary black hole, it introduces a mass distribution  $\rho(x)$  smeared over a

region with a characteristic size of about  $r_b$ , and cannot be approximated as a point mass. When the bosons transfer from the primary black hole to the companion black hole and the cloud consequently depletes, the mass distribution is changed. This leads to a change in the quadrupole moment and thus alters the gravitational wave signal.

To illustrate the effects of mass transfer and cloud depletion, we calculate the difference in average radiation power, denoted as  $\Delta P$ , between the binary black hole system with a boson cloud and the system without a boson cloud. In the BH-cloud-BH system, we assume that before the mass transfer occurs, the two black holes have the same mass  $M$ , and the mass of the boson cloud is  $M_{c,0} = \alpha M$ . For a fair comparison, in the binary black hole system without a boson cloud, we assume that the primary black hole has mass  $(1 + \alpha)M$  and the companion black hole has mass  $M$ . In the parameter regime we consider, it is reasonable to assume that mass transfer occurs at an orbital separation smaller than  $R = 80r_b$ . Furthermore, we assume that the BH-cloud-BH system has the same orbital frequency as the binary black hole system without a boson cloud at the same orbital separation, which leads to a negligible error due to the angular momentum transfer.

Figure 8 shows the ratio between  $\Delta P$  and  $P_0$  for  $\alpha = 0.1$  and  $\alpha = 0.05$ . Before the mass transfer occurs, the power radiated by the BH-cloud-BH system is slightly higher. This is because the extended mass distribution of the boson cloud leads to a larger quadrupole moment and consequently a larger third time derivative, contributing to a slightly higher radiated power. During the mass transfer and cloud depletion, the ratio  $\Delta P/P_0$  decreases gradually due to the redistribution of mass. After the bosons have been completely absorbed, the ratio tends to be a constant. This is because in the final stage, the binary black hole system consists of two black holes with different masses and is devoid of bosons.

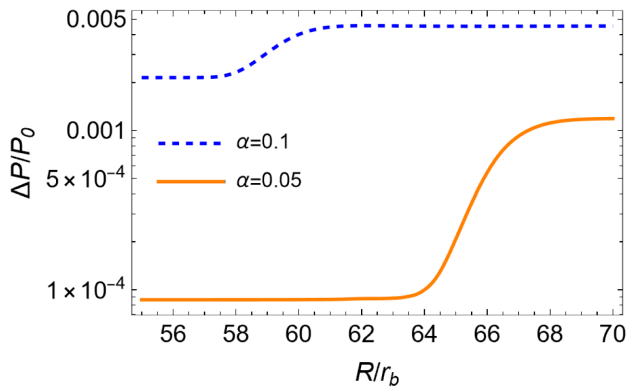


FIG. 8. Ratio between the difference of radiation power,  $\Delta P$ , and the radiation power from a binary black hole system without a boson cloud,  $P_0$ . The blue dashed line and yellow thick line represent bosons with  $\alpha = 0.1$  and  $0.05$ , respectively.

## V. CONCLUSIONS

We develop a framework to study the transfer of bosons between two black holes in a binary black hole system. The framework is formulated by an analogy between the BH-cloud-BH system and the hydrogen molecule ion system in which an electron moves in the potential generated by two protons. When two black holes are sufficiently close, the bosons initially confined around the primary black hole can escape to the companion. In the language of quantum mechanics, molecular orbits of the boson form and the boson moves back and forth between two black holes. This results in cloud mass redistribution in the binary black hole system. Furthermore, the boson which escapes to the companion may occupy the decaying mode and therefore may decay into the companion black hole. We find that the boson cloud existing right before the mass transfer completely disappears. This introduces a new mechanism of cloud depletion in a binary black system distinct from the hyperfine and Bohr mixings. During the evolution of the binary black hole system, the companion first excites the hyperfine mixing, which leads to transitions of bosons between growing and decaying modes, ultimately resulting in depletion to the primary black hole. The cloud depletion progresses slowly until the mass transfer occurs; however, a significant fraction of bosons may have already been absorbed by the primary black hole. The remaining bosons then depletes via mass transfer to the companion black hole.

In this work, we have exclusively focused on scalar bosons without interactions with themselves or other fields. The developed framework can also be applied to bosonic fields with higher spins, e.g., spin-1 [34,53] and spin-2 [31–33] bosonic fields. For vector bosonic fields, the fastest growing mode is the ground state ( $n = 1$ ), rather than the mode  $n = 2, l = m = 1$ , and the growing/decaying rates can be orders of magnitude higher than those of the scalar bosonic fields [53]. This implies that molecular orbits formed by linearly combining two ground states need to be considered, and the vector boson cloud would deplete much more rapidly. If self-interactions exist [25], the bosons can occupy other growing modes with  $n > 2$  and reach a quasiequilibrium configuration [54]. Therefore, molecular orbits with  $n > 2$  have to be considered, leading to earlier mass transfer and cloud depletion through additional decaying channels. If interactions with other fields exist, e.g., axion-photon coupling [55], the transferring bosons can generate or modify visible fields around the companion black hole, potentially producing observable effects.

Our framework is used to study the simplest model where the two black holes have the same mass and spin, and their spin orientation is parallel. It can be straightforwardly generalized to explore more realistic models, for example, the two black holes may have unequal mass and spin, or their spin orientation may be different. This would

require a modification to the variational method used to calculate the molecular orbits and the energy eigenvalues. Another interesting case is that the companion may not be a black hole but a compact star [48]. Then there is only cloud mass redistribution but no cloud depletion due to the decay into the companion. However, this could also have important consequences to the evolution of the binary system and their gravitational waveforms. The boson cloud depletion due to the mass transfer to a companion black hole and that due to the tidal perturbation from the companion [35,56–58] is crucial to understand the dynamics of the boson cloud and to constraint the properties of the ultralight boson.

### ACKNOWLEDGMENTS

D.S. is supported by the Fundamental Research Funds for the Central Universities, HUST (Grant No. 5003012068) and Wuhan Young Talent Research Funds (Grant No. 0106012013). Y.M. is supported by the University start-up funding provided by Huazhong University of Science and Technology.

### APPENDIX A: CHOICE OF COORDINATES

To describe the orbits of the boson in the binary black hole system, we need to set up an appropriate coordinate system, which is schematically shown in Fig. 1. The origin of the coordinate system is located at the primary black hole, and the  $z$ -axis is parallel to the spin of the primary black hole and the  $x$ -axis is pointing towards the companion black hole. We use spherical coordinates  $(r_1, \theta_1, \varphi_1)$  to represent the position of the boson relative to the primary black hole, and  $(r_2, \theta_2, \varphi_2)$  to denote the position of the boson relative to the companion black hole. Whilst one set of coordinates is sufficient, we introduce the coordinates  $(r_2, \theta_2, \varphi_2)$  only for convenience since the isolated wave functions of the boson belonging to the companion black hole can be conveniently expressed using the coordinates  $(r_2, \theta_2, \varphi_2)$ . The coordinates  $(r_2, \theta_2, \varphi_2)$  can be written in terms of the coordinates  $(r_1, \theta_1, \varphi_1)$ ,

$$\begin{aligned} r_2 &= \sqrt{r_1^2 + R^2 - 2r_1R \sin \theta_1 \cos \varphi_1}, \\ \cos \theta_2 &= \frac{r_1 \cos \theta_1}{r_2}, \\ \sin \theta_2 &= \sqrt{1 - (\cos \theta_2)^2}, \\ \cos \varphi_2 &= \frac{r_1 \sin \theta_1 \cos \varphi_1 - R}{r_2 \sin \theta_2}, \\ \sin \varphi_2 &= \frac{r_1 \sin \theta_1 \sin \varphi_1}{r_2 \sin \theta_2}. \end{aligned} \quad (\text{A1})$$

By using these relations we can carry out all the calculation using only one set of coordinates, namely, the coordinates  $(r_1, \theta_1, \varphi_1)$ .

### APPENDIX B: WAVE FUNCTIONS AND OVERLAP INTEGRALS

The wave functions for the  $n = 2, \ell = 1$  boson around an isolated black hole are given by

$$\begin{aligned} \varphi_{2,1,1}(\mathbf{r}) &= \frac{1}{8} \sqrt{\frac{1}{\pi}} r_b^{-5/2} r e^{-r/2r_b} \sin \theta e^{i\varphi}, \\ \varphi_{2,1,-1}(\mathbf{r}) &= \frac{1}{8} \sqrt{\frac{1}{\pi}} r_b^{-5/2} r e^{-r/2r_b} \sin \theta e^{-i\varphi}, \\ \varphi_{2,1,0}(\mathbf{r}) &= \frac{1}{8} \sqrt{\frac{2}{\pi}} r_b^{-5/2} r e^{-r/2r_b} \cos \theta, \end{aligned} \quad (\text{B1})$$

where  $\mathbf{r} = (r, \theta, \varphi)$  and  $r_b$  is the Bohr radius of the boson. It is convenient to define  $\varphi_{2p_x}, \varphi_{2p_y}$ , and  $\varphi_{2p_z}$  states by linearly combining the  $\varphi_{21m}$  states,

$$\begin{aligned} \varphi_{2p_x}(\mathbf{r}) &= \frac{1}{\sqrt{2}} [\varphi_{2,1,1}(\mathbf{r}) + \varphi_{2,1,-1}(\mathbf{r})] \\ &= \frac{1}{8} \sqrt{\frac{2}{\pi}} r_b^{-5/2} r e^{-r/2r_b} \sin \theta \cos \varphi \\ &= \frac{1}{8} \sqrt{\frac{2}{\pi}} r_b^{-5/2} e^{-r/2r_b} x, \end{aligned}$$

$$\begin{aligned} \varphi_{2p_y}(\mathbf{r}) &= \frac{1}{\sqrt{2}i} [\varphi_{2,1,1}(\mathbf{r}) - \varphi_{2,1,-1}(\mathbf{r})] \\ &= \frac{1}{8} \sqrt{\frac{2}{\pi}} r_b^{-5/2} r e^{-r/2r_b} \sin \theta \sin \varphi, \\ &= \frac{1}{8} \sqrt{\frac{2}{\pi}} r_b^{-5/2} e^{-r/2r_b} y, \end{aligned}$$

$$\begin{aligned} \varphi_{2p_z}(\mathbf{r}) &= \frac{1}{8} \sqrt{\frac{2}{\pi}} r_b^{-5/2} r e^{-r/2r_b} \cos \theta \\ &= \frac{1}{8} \sqrt{\frac{2}{\pi}} r_b^{-5/2} e^{-r/2r_b} z. \end{aligned}$$

It is evident that the wave functions  $\varphi_{2p_x}, \varphi_{2p_y}$  and  $\varphi_{2p_z}$  are real, and they are invariant under the rotation along the  $x$ -axis,  $y$ -axis and  $z$ -axis, respectively. These symmetric properties are important for the construction of molecular orbits using the variational method.

The wave functions for the molecular orbits of the boson in the binary black hole system are given by

$$\begin{aligned}
 \varphi_\sigma(\mathbf{r}) &= \frac{1}{8N_1} \sqrt{\frac{1}{\pi}} \left( r_{b1}^{-5/2} r_1 e^{-r_1/2r_{b1}} \sin \theta_1 \cos \varphi_1 - r_{b2}^{-5/2} r_2 e^{-r_2/2r_{b2}} \sin \theta_2 \cos \varphi_2 \right), \\
 \varphi_{\sigma^*}(\mathbf{r}) &= \frac{1}{8N_2} \sqrt{\frac{1}{\pi}} \left( r_{b1}^{-5/2} r_1 e^{-r_1/2r_{b1}} \sin \theta_1 \cos \varphi_1 + r_{b2}^{-5/2} r_2 e^{-r_2/2r_{b2}} \sin \theta_2 \cos \varphi_2 \right), \\
 \varphi_\pi(\mathbf{r}) &= \frac{1}{8N_3} \sqrt{\frac{1}{\pi}} \left( r_{b1}^{-5/2} r_1 e^{-r_1/2r_{b1}} \sin \theta_1 \sin \varphi_1 + r_{b2}^{-5/2} r_2 e^{-r_2/2r_{b2}} \sin \theta_2 \sin \varphi_2 \right), \\
 \varphi_{\pi^*}(\mathbf{r}) &= \frac{1}{8N_4} \sqrt{\frac{1}{\pi}} \left( r_{b1}^{-5/2} r_1 e^{-r_1/2r_{b1}} \sin \theta_1 \sin \varphi_1 - r_{b2}^{-5/2} r_2 e^{-r_2/2r_{b2}} \sin \theta_2 \sin \varphi_2 \right),
 \end{aligned} \tag{B2}$$

where  $r_{b1}$  and  $r_{b2}$  are the Bohr radius for the boson in primary and companion black holes, respectively. The overlap integrals are given by

$$\begin{aligned}
 \langle \varphi_{2p_x}^1 | \varphi_{2p_x}^2 \rangle &= \frac{1}{32\pi} r_{b1}^{-5/2} r_{b2}^{-5/2} \int r_1^3 r_2 e^{-\frac{r_1}{2r_{b1}} - \frac{r_2}{2r_{b2}}} \sin^2 \theta_1 \sin \theta_2 \cos \varphi_1 \cos \varphi_2 dr_1 d\theta_1 d\varphi_1, \\
 \langle \varphi_{2p_x}^1 | \frac{\alpha}{r_2} | \varphi_{2p_x}^2 \rangle &= \frac{\alpha}{32\pi} r_{b1}^{-5/2} r_{b2}^{-5/2} \int r_1^3 e^{-\frac{r_1}{2r_{b1}} - \frac{r_2}{2r_{b2}}} \sin^2 \theta_1 \sin \theta_2 \cos \varphi_1 \cos \varphi_2 dr_1 d\theta_1 d\varphi_1, \\
 \langle \varphi_{2p_x}^1 | \frac{\alpha}{r_2} | \varphi_{2p_x}^1 \rangle &= \frac{\alpha}{32\pi} r_{b1}^{-5} \int \frac{r_1^4}{r_2} e^{-\frac{r_1}{r_{b1}}} \sin^3 \theta_1 \cos^2 \varphi_1 dr_1 d\theta_1 d\varphi_1, \\
 \langle \varphi_{2p_y}^1 | \varphi_{2p_y}^2 \rangle &= \frac{1}{32\pi} r_{b1}^{-5/2} r_{b2}^{-5/2} \int r_1^3 r_2 e^{-\frac{r_1}{2r_{b1}} - \frac{r_2}{2r_{b2}}} \sin^2 \theta_1 \sin \theta_2 \sin \varphi_1 \sin \varphi_2 dr_1 d\theta_1 d\varphi_1, \\
 \langle \varphi_{2p_y}^1 | \frac{\alpha}{r_2} | \varphi_{2p_y}^2 \rangle &= \frac{\alpha}{32\pi} r_{b1}^{-5/2} r_{b2}^{-5/2} \int r_1^3 e^{-\frac{r_1}{2r_{b1}} - \frac{r_2}{2r_{b2}}} \sin^2 \theta_1 \sin \theta_2 \sin \varphi_1 \sin \varphi_2 dr_1 d\theta_1 d\varphi_1, \\
 \langle \varphi_{2p_y}^1 | \frac{\alpha}{r_2} | \varphi_{2p_y}^1 \rangle &= \frac{\alpha}{32\pi} r_{b1}^{-5} \int \frac{r_1^4}{r_2} e^{-\frac{r_1}{r_{b1}}} \sin^3 \theta_1 \sin^2 \varphi_1 dr_1 d\theta_1 d\varphi_1.
 \end{aligned} \tag{B3}$$

### APPENDIX C: QUANTUM ADIABATIC THEOREM

In this appendix, we show that the adiabatic approximation can be applied in our case. Since the potential generated by the two black holes changes very slowly, we assume that the energy eigenvalues also evolve slowly and continuously with time and they satisfy the equation,

$$\hat{H}(t)|\psi_n(t)\rangle = E_n(t)|\psi_n(t)\rangle. \tag{C1}$$

We assume that the energy levels are not degenerate. An arbitrary state at a given time can be written as

$$|\psi(t)\rangle = \sum_n c_n(t) |\psi_n(t)\rangle, \tag{C2}$$

and satisfies the Schrödinger equation

$$i \frac{\partial}{\partial t} |\psi(t)\rangle = \hat{H}(t) |\psi(t)\rangle, \tag{C3}$$

By substituting Eq. (C2) into Eq. (C3), and multiplying both sides from the left by  $\langle \psi_k |$ , we have

$$i \frac{\partial c_k}{\partial t} + i \sum_n c_n \langle \psi_k | \frac{\partial \psi_n}{\partial t} \rangle = c_k E_k. \tag{C4}$$

Now we are going to derive the expression for  $\langle \psi_k | \frac{\partial \psi_n}{\partial t} \rangle$ . We start with a time derivation of Eq. (C1),

$$\frac{\partial \hat{H}}{\partial t} |\psi_n\rangle + \hat{H} \left| \frac{\partial \psi_n}{\partial t} \right\rangle = \frac{\partial E_n}{\partial t} |\psi_n\rangle + E_n \left| \frac{\partial \psi_n}{\partial t} \right\rangle. \tag{C5}$$

For  $k \neq n$ , we multiply both sides from the left by  $\langle \psi_k |$  and obtain,

$$\langle \psi_k | \frac{\partial \psi_n}{\partial t} \rangle = \frac{1}{E_n - E_k} \langle \psi_k | \frac{\partial \hat{H}}{\partial t} | \psi_n \rangle. \tag{C6}$$

We also need to consider the case when  $k = n$ , namely, the expression for  $\langle \psi_k | \frac{\partial \psi_k}{\partial t} \rangle$ . Taking time derivative of the normalization condition,

$$\langle \psi_k | \psi_k \rangle = 1, \tag{C7}$$

we have

$$\langle \psi_k | \frac{\partial \psi_k}{\partial t} \rangle + \langle \frac{\partial \psi_k}{\partial t} | \psi_k \rangle = 0. \tag{C8}$$

It is evident that  $\langle \psi_k | \frac{\partial \psi_k}{\partial t} \rangle$  is purely imaginary, which in principle can be canceled by appropriately adding a phase. Therefore, the time derivative of the coefficient  $c_n$  is given by

$$\frac{dc_k}{dt} = - \sum_{n \neq k} c_n \frac{1}{E_n - E_k} \langle \psi_k | \frac{\partial \hat{H}}{\partial t} | \psi_n \rangle - ic_k E_k. \quad (\text{C9})$$

We now show that  $\langle \psi_k | \frac{\partial \hat{H}}{\partial t} | \psi_n \rangle = 0$  when  $n \neq k$ , which is the equality given by Eq. (23). Since  $n, k \in \{\sigma, \sigma^*, \pi, \pi^*\}$ , so there are six off-diagonal elements for  $\frac{\partial \hat{H}}{\partial t}$ . Let us first consider  $\langle \sigma | \frac{\partial \hat{H}}{\partial t} | \sigma^* \rangle$  and  $\langle \pi | \frac{\partial \hat{H}}{\partial t} | \pi^* \rangle$ .

$$\begin{aligned} \langle \sigma | \frac{\partial \hat{H}}{\partial t} | \sigma^* \rangle &= \langle \varphi_{2p_x}^1 | \frac{\partial \hat{H}}{\partial t} | \varphi_{2p_x}^1 \rangle - \langle \varphi_{2p_x}^2 | \frac{\partial \hat{H}}{\partial t} | \varphi_{2p_x}^2 \rangle \\ &\quad + \langle \varphi_{2p_x}^1 | \frac{\partial \hat{H}}{\partial t} | \varphi_{2p_x}^2 \rangle - \langle \varphi_{2p_x}^2 | \frac{\partial \hat{H}}{\partial t} | \varphi_{2p_x}^1 \rangle. \end{aligned} \quad (\text{C10})$$

In our simple model we assume that two black holes have exactly the same parameters, so the isolated orbits of the boson are the same for the primary and companion black holes. Due to the symmetry of the configuration of the BH-cloud-BH system, we have  $\langle \varphi_{2p_x}^1 | \frac{\partial \hat{H}}{\partial t} | \varphi_{2p_x}^1 \rangle = \langle \varphi_{2p_x}^2 | \frac{\partial \hat{H}}{\partial t} | \varphi_{2p_x}^2 \rangle$ . The wave functions  $\varphi_{2p_x}^i$  are real and the time derivative of the Hamiltonian is Hermitian, so we have  $\langle \varphi_{2p_x}^1 | \frac{\partial \hat{H}}{\partial t} | \varphi_{2p_x}^2 \rangle = \langle \varphi_{2p_x}^2 | \frac{\partial \hat{H}}{\partial t} | \varphi_{2p_x}^1 \rangle$ . Therefore, we find that  $\langle \sigma | \frac{\partial \hat{H}}{\partial t} | \sigma^* \rangle = 0$ . By using similar arguments we also have  $\langle \pi | \frac{\partial \hat{H}}{\partial t} | \pi^* \rangle = 0$ .

To calculate other elements of  $\frac{\partial \hat{H}}{\partial t}$ , we need to know its explicit expression, which is given by

$$\begin{aligned} \frac{\partial \hat{H}}{\partial t} &= \frac{\partial \hat{H}}{\partial r_2} \frac{\partial r_2}{\partial R} \frac{\partial R}{\partial t} = \frac{\alpha}{r_2^2} \frac{\partial r_2}{\partial R} \frac{\partial R}{\partial t} \\ &= -\frac{64}{5} \alpha q (1+q) \frac{M^3 R - r_1 \sin \theta_1 \cos \varphi_1}{R^3 r_2^3}. \end{aligned} \quad (\text{C11})$$

By using the explicit expressions of the orbits given by Eqs. (5) and (6), we find that other elements of  $\frac{\partial \hat{H}}{\partial t}$  can be expanded using  $\langle \varphi_{2p_x}^i | \frac{\partial \hat{H}}{\partial t} | \varphi_{2p_y}^j \rangle$ , with  $i, j \in \{1, 2\}$ . We now show that  $\langle \varphi_{2p_x}^i | \frac{\partial \hat{H}}{\partial t} | \varphi_{2p_y}^j \rangle = 0$  for all choices of  $i, j$ .

Neglecting the constant factor that is independent of  $(r_1, \theta_1, \varphi_1)$  we find,

$$\begin{aligned} &\langle \varphi_{2p_x}^1 | \frac{\partial \hat{H}}{\partial t} | \varphi_{2p_y}^1 \rangle \\ &\sim \int dV \frac{R - r_1 \sin \theta_1 \cos \varphi_1}{r_2^3} r_1^2 e^{-r_1/r_b} \sin^2 \theta_1 \sin \varphi_1 \cos \varphi_1 \\ &\sim \int dx dy dz \frac{x(R-x)y}{(r_1^2 + R^2 - 2Rx)^{3/2}} e^{-r_1/r_b}, \end{aligned} \quad (\text{C12})$$

where we have used the Cartesian coordinates  $(x, y, z)$ ,

$$x = r_1 \sin \theta_1 \cos \varphi_1, \quad y = r_1 \sin \theta_1 \sin \varphi_1, \quad z = r_1 \cos \theta_1.$$

It is evident that the integrand is an odd function of  $y$ , so the integral is zero,

$$\begin{aligned} &\langle \varphi_{2p_x}^1 | \frac{\partial \hat{H}}{\partial t} | \varphi_{2p_y}^2 \rangle \\ &\sim \int dV \frac{R - r_1 \sin \theta_1 \cos \varphi_1}{r_2^3} e^{-(r_1+r_2)/2r_b} r_1 \sin \theta_1 \cos \varphi_1 \\ &\quad \times r_2 \sin \theta_2 \sin \varphi_2 \\ &\sim \int dx dy dz \frac{x(R-x)y}{(r_1^2 + R^2 - 2Rx)^{3/2}} e^{-(r_1+r_2)/2r_b}, \end{aligned} \quad (\text{C13})$$

where  $r_2 = \sqrt{r_1^2 + R^2 - 2Rx}$ , and we have used the equality  $y = r_1 \sin \theta_1 \cos \varphi_1 = r_2 \sin \theta_2 \cos \varphi_2$ . It is evident that the integrand is also an odd function of  $y$ , so the integral is zero.

By using the symmetry of the BH-cloud-BH system, we have

$$\begin{aligned} \langle \varphi_{2p_x}^2 | \frac{\partial \hat{H}}{\partial t} | \varphi_{2p_y}^1 \rangle &= -\langle \varphi_{2p_x}^1 | \frac{\partial \hat{H}}{\partial t} | \varphi_{2p_y}^2 \rangle = 0, \\ \langle \varphi_{2p_x}^2 | \frac{\partial \hat{H}}{\partial t} | \varphi_{2p_y}^2 \rangle &= -\langle \varphi_{2p_x}^1 | \frac{\partial \hat{H}}{\partial t} | \varphi_{2p_y}^1 \rangle = 0. \end{aligned} \quad (\text{C14})$$

Therefore, We have  $\langle \varphi_{2p_x}^i | \frac{\partial \hat{H}}{\partial t} | \varphi_{2p_y}^j \rangle = 0$  for all choices of  $i, j$ . As a result, all other elements of  $\frac{\partial \hat{H}}{\partial t}$  are zero. In summary, we have

$$\langle \psi_k | \frac{\partial \hat{H}}{\partial t} | \psi_n \rangle = 0 \quad (\text{C15})$$

for  $n \neq k$ .

- [1] B. P. Abbott, R. Abbott, T. D. Abbott, M. R. Abernathy, F. Acernese, K. Ackley, C. Adams, T. Adams, P. Addesso, R. X. Adhikari *et al.* (LIGO Scientific and Virgo Collaborations), *Phys. Rev. Lett.* **116**, 061102 (2016).
- [2] F. Acernese, M. Agathos, K. Agatsuma, D. Aisa, N. Allemandou, A. Allocca, J. Amarni, P. Astone, G. Balestri, G. Ballardin *et al.*, *Classical Quantum Gravity* **32**, 024001 (2014).
- [3] Y. Aso, Y. Michimura, K. Somiya, M. Ando, O. Miyakawa, T. Sekiguchi, D. Tatsumi, and H. Yamamoto (The KAGRA Collaboration), *Phys. Rev. D* **88**, 043007 (2013).
- [4] P. Amaro-Seoane, H. Audley, S. Babak, J. Baker, E. Barausse, P. Bender, E. Berti, P. Binetruy, M. Born, D. Bortoluzzi *et al.*, [arXiv:1702.00786](https://arxiv.org/abs/1702.00786).
- [5] J. Luo, L.-S. Chen, H.-Z. Duan, Y.-G. Gong, S. Hu, J. Ji, Q. Liu, J. Mei, V. Milyukov, M. Sazhin *et al.*, *Classical Quantum Gravity* **33**, 035010 (2016).
- [6] W.-R. Hu and Y.-L. Wu, *Natl. Sci. Rev.* **4**, 685 (2017).
- [7] R. D. Peccei and H. R. Quinn, *Phys. Rev. Lett.* **38**, 1440 (1977).
- [8] S. Weinberg, *Phys. Rev. Lett.* **40**, 223 (1978),
- [9] F. Wilczek, *Phys. Rev. Lett.* **40**, 279 (1978).
- [10] P. Svrcek and E. Witten, *J. High Energy Phys.* **06** (2006) 051.
- [11] J. Preskill, M. B. Wise, and F. Wilczek, *Phys. Lett.* **120B**, 127 (1983).
- [12] L. Abbott and P. Sikivie, *Phys. Lett.* **120B**, 133 (1983).
- [13] M. Dine and W. Fischler, *Phys. Lett.* **120B**, 137 (1983).
- [14] B. Li, T. Rindler-Daller, and P. R. Shapiro, *Phys. Rev. D* **89**, 083536 (2014).
- [15] L. Hui, J. P. Ostriker, S. Tremaine, and E. Witten, *Phys. Rev. D* **95**, 043541 (2017).
- [16] Y. B. Zel'Dovich, *JETP Lett.* **14**, 180 (1971).
- [17] Y. B. Zel'Dovich, *JETP Lett.* **35**, 1085 (1972).
- [18] C. Misner, *Bull. Am. Phys. Soc.* **17**, 472 (1972).
- [19] A. A. Starobinskiĭ, *JETP Lett.* **37**, 28 (1973).
- [20] A. A. Starobinskiĭ and S. M. Churilov, *JETP Lett.* **38**, 1 (1974).
- [21] W. E. East and F. Pretorius, *Phys. Rev. Lett.* **119**, 041101 (2017),
- [22] W. E. East, *Phys. Rev. D* **96**, 024004 (2017),
- [23] R. Brito, V. Cardoso, and P. Pani, *Superradiance* (Springer, New York, 2020), Vol. 10.
- [24] M. Cromb, G. M. Gibson, E. Toninelli, M. J. Padgett, E. M. Wright, and D. Faccio, *Nat. Phys.* **16**, 1069 (2020).
- [25] A. Arvanitaki and S. Dubovsky, *Phys. Rev. D* **83**, 044026 (2011),
- [26] R. Brito, S. Ghosh, E. Barausse, E. Berti, V. Cardoso, I. Dvorkin, A. Klein, and P. Pani, *Phys. Rev. D* **96**, 064050 (2017).
- [27] A. Arvanitaki, M. Baryakhtar, and X. Huang, *Phys. Rev. D* **91**, 084011 (2015).
- [28] A. Arvanitaki, S. Dimopoulos, S. Dubovsky, N. Kaloper, and J. March-Russell, *Phys. Rev. D*, 123530 **81** (2010).
- [29] K. K. Y. Ng, S. Vitale, O. A. Hannuksela, and T. G. F. Li, *Phys. Rev. Lett.* **126**, 151102 (2021).
- [30] L. Tsukada, R. Brito, W. E. East, and N. Siemonsen, *Phys. Rev. D* **103**, 083005 (2021).
- [31] R. Brito, S. Grillo, and P. Pani, *Phys. Rev. Lett.* **124**, 211101 (2020).
- [32] O. J. C. Dias, G. Lingetti, P. Pani, and J. E. Santos, *Phys. Rev. D* **108**, L041502 (2023).
- [33] W. E. East and N. Siemonsen, *Phys. Rev. D* **108**, 124048 (2023).
- [34] N. Siemonsen and W. E. East, *Phys. Rev. D* **101**, 024019 (2020).
- [35] D. Baumann, H. S. Chia, and R. A. Porto, *Phys. Rev. D* **99**, 044001 (2019).
- [36] T. Takahashi, H. Omiya, and T. Tanaka, *Prog. Theor. Exp. Phys.* **2022**, 043E01 (2022).
- [37] J. Zhang and H. Yang, *Phys. Rev. D* **99**, 064018 (2019).
- [38] Q. Ding, X. Tong, and Y. Wang, *Astrophys. J.* **908**, 78 (2021).
- [39] X. Tong, Y. Wang, and H.-Y. Zhu, *Astrophys. J.* **924**, 99 (2022).
- [40] E. Berti, R. Brito, C. F. B. Macedo, G. Raposo, and J. L. Rosa, *Phys. Rev. D* **99**, 104039 (2019).
- [41] T. Takahashi and T. Tanaka, *J. Cosmol. Astropart. Phys.* **10** (2021) 031.
- [42] T. Takahashi, H. Omiya, and T. Tanaka, *Phys. Rev. D* **107**, 103020 (2023).
- [43] D. Baumann, G. Bertone, J. Stout, and G. M. Tomaselli, *Phys. Rev. Lett.* **128**, 221102 (2022).
- [44] N. Siemonsen, T. May, and W. E. East, *Phys. Rev. D* **107**, 104003 (2023).
- [45] L. K. Wong, *Phys. Rev. D* **101**, 124049 (2020).
- [46] T. Ikeda, L. Bernard, V. Cardoso, and M. Zilhão, *Phys. Rev. D* **103**, 024020 (2021).
- [47] S. Detweiler, *Phys. Rev. D* **22**, 2323 (1980).
- [48] T. Liu and K.-F. Lyu, [arXiv:2107.09971](https://arxiv.org/abs/2107.09971).
- [49] C. Cohen-Tannoudji, B. Diu, and F. Laloe, *Quantum Mech.* **2**, 626 (1986).
- [50] P. C. Peters, *Phys. Rev.* **136**, B1224 (1964).
- [51] S. R. Dolan, *Phys. Rev. D* **76**, 084001 (2007).
- [52] H. Yoshino and H. Kodama, *Prog. Theor. Exp. Phys.* **2014**, 043E02 (2014).
- [53] M. Baryakhtar, R. Lasenby, and M. Teo, *Phys. Rev. D* **96**, 035019 (2017).
- [54] M. Baryakhtar, M. Galanis, R. Lasenby, and O. Simon, *Phys. Rev. D* **103**, 095019 (2021).
- [55] N. Siemonsen, C. Mondino, D. Egaña Ugrinovic, J. Huang, M. Baryakhtar, and W. E. East, *Phys. Rev. D* **107**, 075025 (2023).
- [56] X. Tong, Y. Wang, and H.-Y. Zhu, *Phys. Rev. D* **106**, 043002 (2022).
- [57] V. D. Luca and P. Pani, *J. Cosmol. Astropart. Phys.* **08** (2021) 032.
- [58] V. De Luca, A. Maselli, and P. Pani, *Phys. Rev. D* **107**, 044058 (2023).